The Importance of Thermospheric Winds for Ionospheric Modeling

A White Paper for the Decadal Survey of Solar and Space Physics

Sarah E. McDonald, Douglas P. Drob, John Emmert, Christoph Englert, David Siskind
Space Science Division, Naval Research Laboratory, Washington, DC

Joseph Huba, Jonathan Krall
Plasma Physics Division, Naval Research Laboratory, Washington, DC

Sunanda Basu
Institute for Scientific Research, Boston College, Chestnut Hill, MA

Introduction and Motivation

One of the most fundamental Heliophysical processes is the coupling between charged and neutral particles. In the presence of a magnetic field, drag forces between the charged and neutral gases produce complex electrodynamic interactions. Understanding these interactions was listed as one of the three key research focus areas in the recent Heliophysics Roadmap for enabling space environmental prediction. In the terrestrial environment, these ion-neutral interactions are most vividly manifest in the low latitude ionosphere. Specifically variations in the neutral wind can drive a complex system of ionospheric currents and electric fields, which in turn profoundly influence the structure and composition of the ionosphere. Recent observations have suggested new and previously unknown ionospheric morphologies, which have been linked to neutral wind variability. State-of-the-art coupled thermosphere-ionosphere-electrodynamics models make specific predictions for ion-neutral coupling based upon this variability; however, these theories remain untested by appropriate global observations. A key stumbling block is the lack of neutral winds with sufficient altitudinal and horizontal resolution. Here we present some specific examples where neutral wind measurements are needed to enable reliable ionospheric modeling.

The Wind Dynamo

Winds in the Earth's thermosphere (75 to 500 km) are driven primarily by pressure gradients resulting from temperature differences, with the absorption of solar EUV radiation being the dominant source of heating. Secondary sources of heating arise from collisions between the atmospheric constituents and precipitating energetic auroral particles, and friction resulting from the interaction of neutral gas with magnetospherically driven ion flows at high latitudes. Deposition of energy from the lower atmosphere in the form of upward propagating planetary waves, tides and gravity waves is also important, especially in the lower thermosphere (below 200 km).

The Earth's global wind system contributes significantly to the morphology and variability of the ionosphere. Thermospheric (or neutral) winds blow the ionospheric plasma across the magnetic field, resulting in a separation of charge similar to a dynamo. In the E-region ionosphere (90 – 140 km) the ion-neutral collision frequency is so high that the neutral wind can drag the ions with it, whereas the electrons are constrained to gyrate along the magnetic field and drift transverse to the electric field. Differences in the ion and electron velocities, and small differences in their concentrations are responsible for generating currents and polarization

electric fields in this highly conducting region of the ionosphere. Such electric fields arising from winds in the thermosphere are called dynamo electric fields. Due to the high conductivity along the magnetic field, the E-region dynamo fields map along the magnetic field lines to the F-region (140 – 500 km) ionosphere. Though the E-region dynamo dominates during the day, ion-neutral interactions in the F-region are responsible for an F-region dynamo that becomes important at night when the E-region conductivity is low.

A key feature of the E-region dynamo is the generation of a zonal (east-west) electric field that drives a vertical $\mathbf{E} \times \mathbf{B}$ drift of F-region plasma at the equator, which is one of the most important processes controlling the large-scale distribution of plasma. To first order, the neutral winds blow from the dayside to the nightside leading to upward plasma drift during the day and downward drift at night. The upward plasma drift at the magnetic equator in combination with ambipolar diffusion along the field lines results in regions of enhanced plasma density on either side of the magnetic equator, referred to as the Equatorial Ionization Anomaly (EIA), an important feature of the low-latitude ionosphere.

A major achievement in the development of global modeling of the thermosphere-ionospheric system in the past two decades has been the incorporation of a self-consistent electrodynamic model. This was first achieved with the Thermosphere Ionosphere Electrodynamic General Circulation Model (TIEGCM) (Richmond et al., 1992). Using TIEGCM, Fesen et al. (2000) was able to successfully model the key features of the $\mathbf{E} \times \mathbf{B}$ drift. However, there is still much work to be accomplished in modeling the observed day-to-day, longitudinal and seasonal variations of the ionospheric electrodynamics. In fact, there have been a number of new observations of ionospheric phenomena that suggest that the ionosphere-thermosphere (IT) system is much more interesting and complex than previously thought. Longitudinal variation in the morphology of the low-latitude ionosphere has been linked to non-migrating tides of tropospheric origin (Hagan and Forbes, 2003) that drive the E-region dynamo, thus affecting the F-region ionosphere (Immel et al., 2006). Large pre-dawn density depletions in the equatorial ionosphere have been observed below ~550 km (de la Beaujardiere., 2009) and have been attributed to zonal winds (Huba et al, 2010). Chau et al. (2009) found a unique daytime pattern in the vertical $\mathbf{E} \times \mathbf{B}$ drifts over Jicamarca associated with a largescale meteorological disturbance known as a sudden stratospheric warming (SSW) event in January 2008.

The largest hurdle in understanding these phenomena is knowledge of the winds that drive the E- and F-region dynamos. Below, we highlight four important ionospheric phenomena driven by thermospheric winds that require additional modeling in order to be fully understood. We then summarize the thermospheric winds measurements that have been made to date and highlight a new wind instrument concept.

Pre-reversal Enhancement of the Vertical Plasma Drift

At dusk, when the E-region density decreases, the F-region dynamo becomes more significant. The complex interaction of the E- and F-region dynamos causes an enhancement of the eastward electric field (and upward $\mathbf{E} \times \mathbf{B}$ drift) prior to turning westward. Because of the large upward drifts associated with this prereversal enhancement (PRE) of the electric field, it is a significant factor in the development of ionospheric irregularities (or depletions) that can impact communication and navigation systems. A large PRE can lift the F-region ionosphere to high

altitudes, where recombination is slow. At the same time, the E-region ionosphere is quickly depleted in the absence of photoproduction, which sets up the conditions for a gravitational Rayleigh-Taylor instability to form. Small perturbations in the bottomside density can lead to growth of the instability that results in plasma irregularities (i.e. Equatorial Spread F) and the formation of bubbles, which are structures of depleted density that rise up through the F-region ionosphere. Thus, better understanding of the conditions that lead to the development of the PRE will result in improved irregularity forecasting systems.

A number of theories and models have been developed to explain the PRE and are summarized by Eccles (1998). In each case, the main driver of the PRE is the zonal (eastward) F-region neutral wind, but modeling work by Millward et al. (2001) indicates that the E-region neutral winds can modulate the amplitude of the PRE. There are now various ground-and space-based measurements of the F-region vertical plasma drift that show substantial longitudinal and seasonal variations. For example, Fejer et al. (2008) used ROCSAT-1 drift measurements to develop an empirical model that captures the longitudinal and seasonal variation of the plasma drifts. Figure 1 shows the longitudinal and seasonal variation of the PRE. When such drift models are used in ionospheric models, resulting electron densities are often in good agreement with observations (e.g. Fang et al. 2009). However, models that self-consistently calculate the electric fields from neutral wind models have yet to fully capture the observed variations in the vertical plasma drift. Higher resolution wind models at E- and F-region altitudes are needed to fully understand the drivers of the variation in the PRE as well as to validate the ionosphere models.

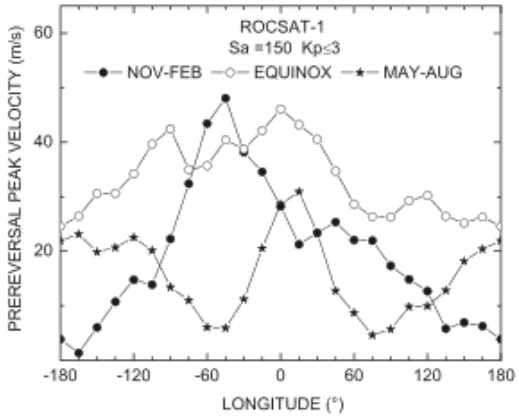

Figure 1. Peak velocity of the PRE as a function of longitude and season. From Fejer et al. (2008).

Ionospheric Irregularity Formation

The strength of the PRE, due to competing dynamo action of winds in the E- and F-region ionosphere, is an important factor in the development of ionospheric irregularities. But the thermospheric winds also play other important roles in the formation and/or suppression of irregularities. Gravity waves have long been suspected to play a role in providing the necessary perturbation to the bottomside of the unstable layer in order to set off an instability (e.g. Fritts et

al., 2009). However, Kudeki et al. (2007) have presented experimental and modeling evidence that F-region eastward neutral winds at sunset play the dominant role in triggering equatorial spread-F. Maruyama and Matuura (1984) predicted that asymmetric density distributions along a flux tube, resulting from interhemispheric F-region winds, can suppress the growth of the Rayleigh-Taylor instability. To test this theory, Krall et al. (2009) used an ionospheric model of ESF (SAMI3/ESF) to show that a constant meridional wind of 60 m s^{-1} stabilizes equatorial spread-F.

Dawn Depletions

Large-scale, dawn density depletions have been recently observed in the equatorial ionosphere during the recent extreme solar minimum conditions (de la Beaujardiere et al., 2009). Simulation results using SAMI3 (Huba et al., 2010) show that the observed depletions can be explained by a post-midnight enhancement of the upward **E** × **B** drift as result of strong eastward winds between 150 and 250 km. Huba et al. (2010) showed that SAMI3, which self-consistently solves for the electric fields, yields two different solutions when driven by two different empirical models of the neutral winds: HWM93 (Hedin et al., 1996) and HWM07 (Drob et al., 2008). As shown in Figure 2, a dawn density depletion forms over South American when the HWM07 wind model is used, but that this depletion is not present with the HWM93 model. A comparison of the wind models suggests that the zonal neutral wind is responsible for the depletion. This study highlights the sensitivity of the ionosphere to different wind models, and that the ionosphere is especially sensitive to winds in the E-region.

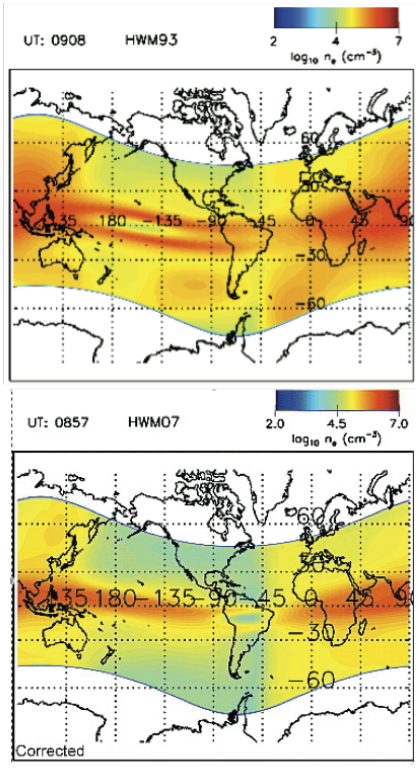

Figure 2. SAMI3 electron density at 0900 UT as a function of geographic latitude and longitude at an altitude of 308 km using (top) HWM93 and (bottom) HWM07. The HWM07 winds produces a density depletion at the magnetic equator over South America. From Huba et al. (2010).

Ionospheric Variability due to Planetary Waves and Tides

Longitudinal variation of the low-latitude ionosphere can in part be attributed to atmospheric nonmigrating tides generated in the lower atmosphere (Immel et al., 2006). Modeling studies have shown that tidal winds can reach significant amplitudes, especially under solar minimum conditions, and that they are significant enough at E-region altitudes to influence the zonal electric fields, and hence the electron densities of the low-latitude F-region ionosphere (Hagan et al., 2007). Recently, Liu et al. (2010) performed numerical simulations to show that planetary waves can cause variability in migrating and nonmigrating tides through nonlinear interactions. The largest changes were found at 100 to 150 km and extended into the upper thermosphere. Their results showed a complex pattern of neutral wind perturbations as a function of time, latitude and longitude.

Wind Measurements

Our understanding of thermospheric winds has historically been limited by a lack of comprehensive measurements. Although tremendous advances in characterizing lower thermospheric (90–120 km) wind patterns have been made as a result of wind measurements by NASA's Upper Atmosphere Research Satellite (UARS) and Thermosphere Ionosphere Mesosphere Energetics and Dynamics (TIMED) missions, winds patterns in the middle thermosphere (120–200 km) are still poorly understood. The Wind Imaging Interferometer (WINDII) on UARS is the only major source of wind measurements in this altitude region (Figure 3). While the WINDII data have afforded significant improvements in our understanding of thermospheric wind patterns, this dataset cannot provide an adequate climatological description of dynamo-generating winds. Between 120 and 200 km the data are limited to daytime only, and the 200–300 km nighttime data are limited to latitudes below 45° and only cover late 1991 to 1994. The UARS mission was designed to study the stratosphere, mesosphere, and lower thermosphere (Reber et al., 1993); the upper thermospheric wind measurements were a supplementary benefit of WINDII, the design of which is optimized primarily for the lower-altitude measurements (Shepherd et al., 1993). Offsets and artifacts in the middle and upper thermospheric WINDII profiles, on the order of 50 m/s (Emmert et al., 2002) impede accurate characterization of average winds.

Archival thermospheric wind measurements as a whole suffer from several key gaps. First, very little is known about nighttime winds between 120 and 200 km. An airglow emission suitable for measurement of Doppler shifts has not been identified, so the only wind data in this region comes from in rocket-borne in situ measurements such as chemical releases. These highly accurate measurements have provided enormously valuable insight into small-scale thermospheric dynamics, but their limited spatial and temporal coverage (about 500 profiles since 1998 [Larsen and Fesen, 2009]) preclude them from contributing significantly to knowledge of global-scale patterns. Another important gap is the availability of wind data during severe geomagnetic storms ($Kp \geq 6$). This is partly a result of the relative rarity of such events; only about 2% of wind measurements have been taken under these conditions. Consequently, our empirical understanding of how winds respond to magnetospheric energy input is very coarse (Emmert et al., 2008), particularly with respect to their development and recovery. To address this deficit, it is essential that we continue building up the wind database for at least several more

solar cycles. Finally, because thermospheric wind patterns are so heavily influenced by upward propagating tides that exhibit significant day-to-day variability, for space weather applications it is critical that winds be continuously monitored at multiple local times. In the upper thermosphere, there is currently very little space-based monitoring of winds (TIMED/TIDI began measuring Doppler shifts of 630.0 nm airglow in late 2008), and contemporary wind measurement coverage is far from sufficient to specify and predict the ionosphere-thermosphere system.

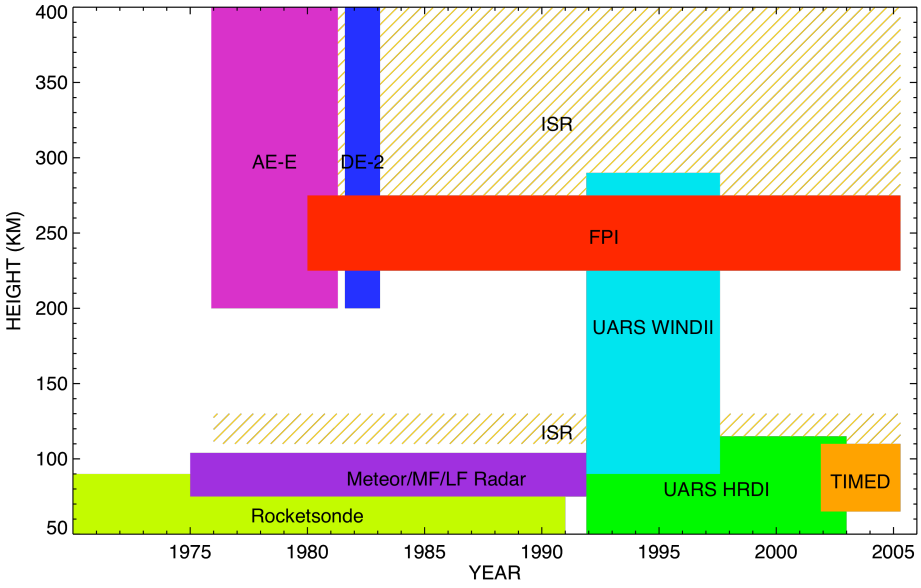

Figure 3. Altitude coverage of major upper atmospheric wind datasets over the past four decades. Most of the datasets shown here are additionally limited in local time and/or latitude. For example the upper thermospheric WINDII measurements are daytime only; ground-based FPI measurements are nighttime only, and the upper thermospheric ISR measurements consist of inferred meridional winds at midlatitudes.

A New Wind Instrument Concept

To provide sufficient input to the ionospheric models, global thermospheric wind measurements with significant spatial resolution are required. Wind profiles encompassing the E- and F-region altitudes are critical. A prime candidate for measuring the thermospheric winds is the Doppler Asymmetric Spatial Heterodyne (DASH) interferometer (Englert et al., 2007). DASH would be capable of measuring thermospheric wind and temperature profiles from low Earth orbit. For the thermosphere, typical measurements could be conducted between 90-300 km altitude with up to 5 km altitude resolution by observing the oxygen red and green lines. With horizontal resolutions of a few hundred kilometers, one can achieve a wind speed precision of less than 5 m/s and temperature precision of less than 5K, depending on the source brightness and altitude resolution. The DASH instrument would also be small and light enough (< 35 kg) to be included even on small missions.

Summary

We have highlighted several important phenomena that impact Earth's ionosphere through the effects of the thermospheric neutral winds. Ionospheric models have reached a level of maturity where improved wind models and/or measurements are needed in order to both validate the models and gain further insight into the physical processes that are being simulated. Thermospheric winds vary considerably with local time, longitude and altitude in the lower thermosphere and have a dramatic effect on the ionosphere. It is therefore critical to promote instruments and new techniques that measure winds with sufficient resolution as well as to develop improved wind models. As a result, our space environment modeling and forecasting capabilities will be greatly enhanced.

References

Chau, J.L., B.G. Fejer, and L.P. Goncharenko, Quiet variability of equatorial E × B drifts during a sudden stratospheric warming event, Geophys. Res. Lett. 36, L05101, doi:10.1029/2008GL036785, 2009.

de La Beaujardiere, O., et al., C/NOFS observations of deep plasma depletions at dawn, Geophys. Res. Lett., 36, L00C06, doi:10.1029/2008JA013668.

Drob, D. P., et al. (2008), An empirical model of the Earth's horizontal wind fields: HWM07, *J. Geophys. Res., 113*, A12304, doi:10.1029/2008JA013668.

Emmert, J. T., B. G. Fejer, G. G. Shepherd, and B. H. Solheim (2002), Altitude dependence of middle and low-latitude daytime thermospheric disturbance winds measured by WINDII, *J. Geophys Res., 107*, doi:10.1029/2002JA009646.

Emmert, J. T., D. P. Drob, G. G. Shepherd, G. Hernandez, M. J. Jarvis, J. W. Meriwether, R. J. Niciejewski, D. P. Sipler, and C. A. Tepley (2008), DWM07 global empirical model of upper thermospheric storm-induced disturbance winds, *J. Geophys Res., 113*, A11319, doi:10.1029/2008JA013541.

Fejer, B. G., J. W. Jensen, and S.-Y. Su (2008), Quiet time equatorial F region vertical plasma drift model derived from ROCSAT-1 observations, *J. Geophys. Res., 113*, A05304, doi:10.1029/2007JA012801.

Fesen, C.G., R.G. Roble, A.D. Richmond, G. Crowley, B.G. Fejer, Simulation of the pre-reversal enhancement in the low-latitude vertical ion drifts, Geophys. Res. Lett, 27, 1851-1854, 2000.

Fritts, D.C., et al. (2009), Overview and summary of the Spread F Experiment (SpreadFEx), *Ann. Geophys*., *27*, 2141-2155.

Hagan, M.E. and J.M. Forbes (2003), Migrating and nonmigrating semi-diurnal tides in the upper atmosphere excited by tropospheric latent heat release, *J. Geophys. Res*., *108*(A2), 1062, doi:10.1029/2002JA009466.

Hagan, M. E, A. Maute, R. G. Roble, A. D. Richmond, T. J. Immel, and S. L. England (2007), Connections between deep tropical clouds and the Earth's ionosphere, *Geophys. Res. Lett., 34*, L20109, doi:10.1029/2007GL030142.

Hedin, A. E., E.L. Fleming, A.H. Manson, F.J. Scmidlin, S.K. Avery, R.R. Clark, S.J. Franke, G.J. Fraser, T. Tsunda, F. Vial and R.A. Vincent (1996), Empirical Wind Model for the Upper, Middle, and Lower Atmosphere, *J. Atmos. Terr. Phys., 58*, 1421.

Huba, J.D., G. Joyce, J. Krall, C.L. Siefring, and P.A. Bernhardt, Self-consistent modeling of equatorial dawn density depletions with SAMI3, Geophys. Res. Lett., 37, L03104, doi:10.1029/2009GL041492, 2010.

Immel, T. J., E. Sagawa, S. L. England, S. B. Henderson, M. E. Hagan, S. B. Mende, H. U. Frey, C. M. Swenson, and L. J. Paxton (2006), Control of equatorial ionospheric morphology by atmospheric tides, *Geophys. Res. Lett., 33*, L15108, doi:10.1029/2006GL026161.

Krall, J., J.D. Huba, G. Joyce, S. Zalesak (2009a), Three-dimensional simulation of equatorial spread-F with meridional wind effects, *Ann. Geophys*., *27*, 1821.

Kudeki, E. Akgiray, A., Milla, M.A., J.L. Chau, and D. Hysell, Equatorial spread-F initiation: post-sunset vortex, thermospheric winds, gravity waves, J. Atmos. Solar Terr. Phys., 69, 2416-2427, 2007.

Larsen, M. F., and C. G. Fesen (2009), Accuracy issues of the existing thermospheric wind models: can we rely on them in seeking solutions to wind-driven problems?, *Ann. Geophys., 27*, 2277–2284.

Liu, H. - L., W. Wang, A. D. Richmond, and R. G. Roble, Ionospheric variability due to planetary waves and tides for solar minimum conditions, J. Geophys. Res., 115, A00G01, doi:10.1029/2009JA015188, 2010.

Maruyama, T., and N. Matuura (1984), Longitudinal variability of annual changes in activity of equatorial spread F and plasma bubbles, *J. Geophys. Res*., *89*, 10903-10912.

Millward, G.H., I.C.F. Muller-Wodarg, A.D. Aylward, T.J. Fuller-Rowell, A.D. Richmond, and R.J. Moffett, An investigation into the influence of tidal forcing on F region equatorial vertical ion drift using a global ionosphere-thermosphere model with coupled electrodynamics, J. Geophys. Res., 106, 24733-24744, 2001.

Reber, C., C. Trevathan, R. McNeal, and M. Luther (1993), The Upper Atmosphere Research Satellite (UARS) mission, *J. Geophys Res., 98*, 10,643–10,647.

Richmond, A.D., E.C. Ridley, and R.G. Roble, A thermosphere/ionosphere general circulation model with coupled electrodynamics, Geophys. Res. Lett., 19, 601-604, 1992.

Shepherd, G. G., et al. (1993), WINDII, the Wind Imaging Interferometer on the Upper Atmosphere Research Satellite, *J. Geophys Res., 98*, 10,725–10,750.